

## ELECTRONIC SUPPLEMENTARY INFORMATION (ESI)

### Enhanced Adhesion and Friction by Electrostatic Interactions of Double-Level Teflon Nanopillars

Hadi Izadi, Mehrnaz Golmakani and Alexander Penlidis\*

\* Corresponding-Author; penlidis@uwaterloo.ca

High aspect-ratio (AR) nanopillars terminated with a fluffy nanostructure on top were fabricated on Teflon AF by infiltration of the polymer melt into an anodic aluminium oxide (AAO) membrane as the mold. The effective elastic modulus ( $E_{eff}$ ) of the 10 fabricated nanopillars can be calculated by<sup>1</sup>

$$E_{eff} = \frac{3EI dsin(\theta)}{L^2 cos^2(\theta)[1 \pm \mu tan(\theta)]} \quad (S1)$$

where  $E$  is the elastic modulus of the polymer,  $I = \pi r^4/4$  ( $r$  is the radius of each hair) the moment of inertia,  $d$  the pillar density,  $L$  the length of each pillar,  $\mu$  the friction coefficient, and  $\theta$  the hair

angle to its base. Considering  $E=1.5$  GPa,<sup>2</sup>  $\mu=0.35$ ,  $\theta=89^\circ$ , and 25% porosity in the mold, which results in  $d=8 \times 10^{12}$  pillars  $m^{-2}$ , the theoretical effective elastic modulus of nanopillars, excluding the hierarchical level, was calculated. For an identical structure, increasing the pillar height (and, consequently, enhancing the AR 70 of pillars) results in lower effective elastic modulus for the fibrillar structure. Lower elastic modulus allows the probe to penetrate deeper into the dry adhesive and thus the number of pillars which come into contact at a specific loading force increases.

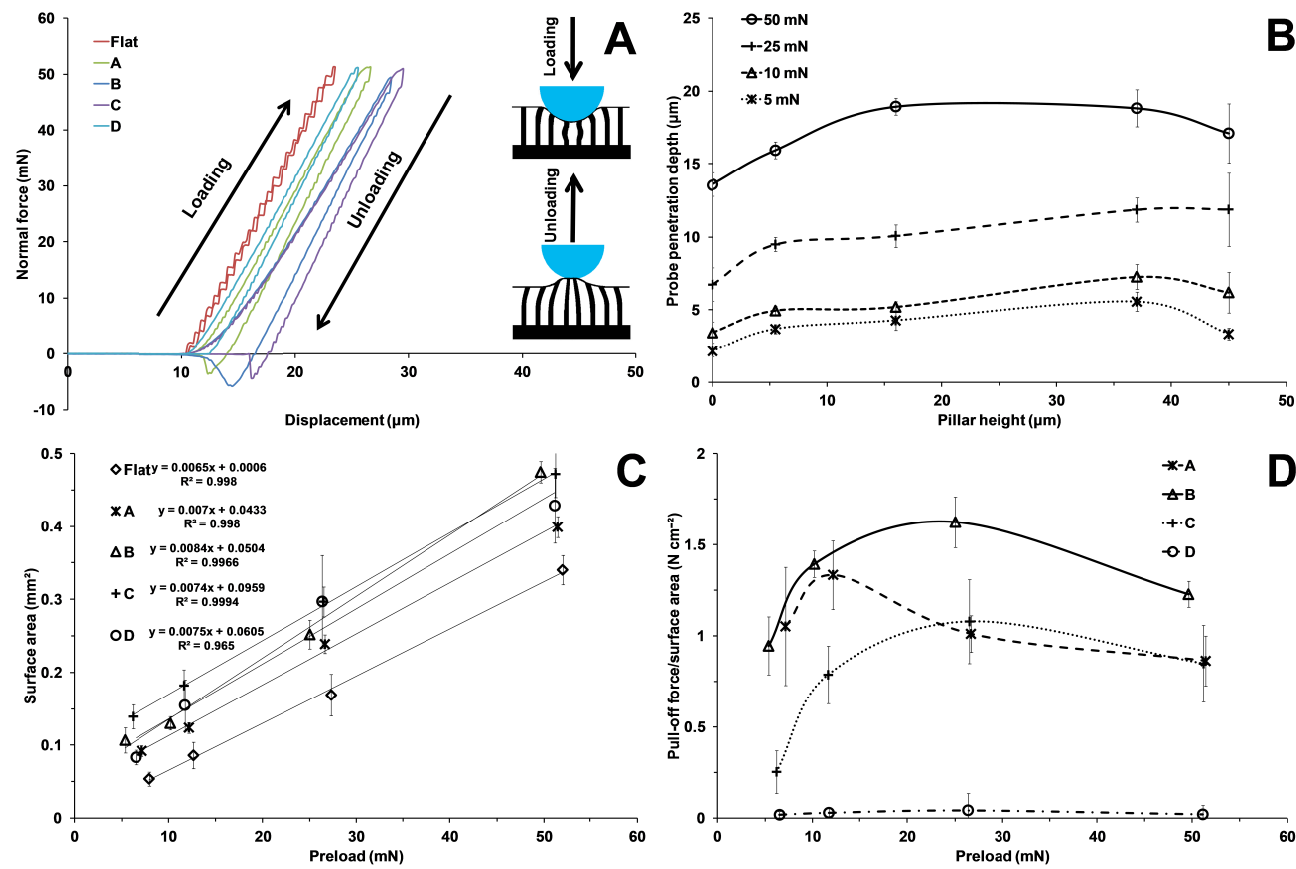


**Fig. S1** (A) Typical force traces (normal force vs. displacement) for different nanopillars of ~5.5, 16, 37, and 45 μm tall (samples A, B, C, and D, respectively) as well as for the flat control samples under a nominal preload of 50 mN. The schematic shows the two steps of loading and unloading in an indentation test with a hemispherical fused silica probe (8 mm in diameter) on double-level Teflon AF nanopillars; (B) Corresponding probe penetration depth, (C) Apparent surface area, and (D) Adhesion strength (i.e., pull-off force per unit surface area) for double-level nanopillars of 200 nm in diameter 30 at nominal preloads of 5, 10, 25, and 50 mN.

## ELECTRONIC SUPPLEMENTARY INFORMATION (ESI)

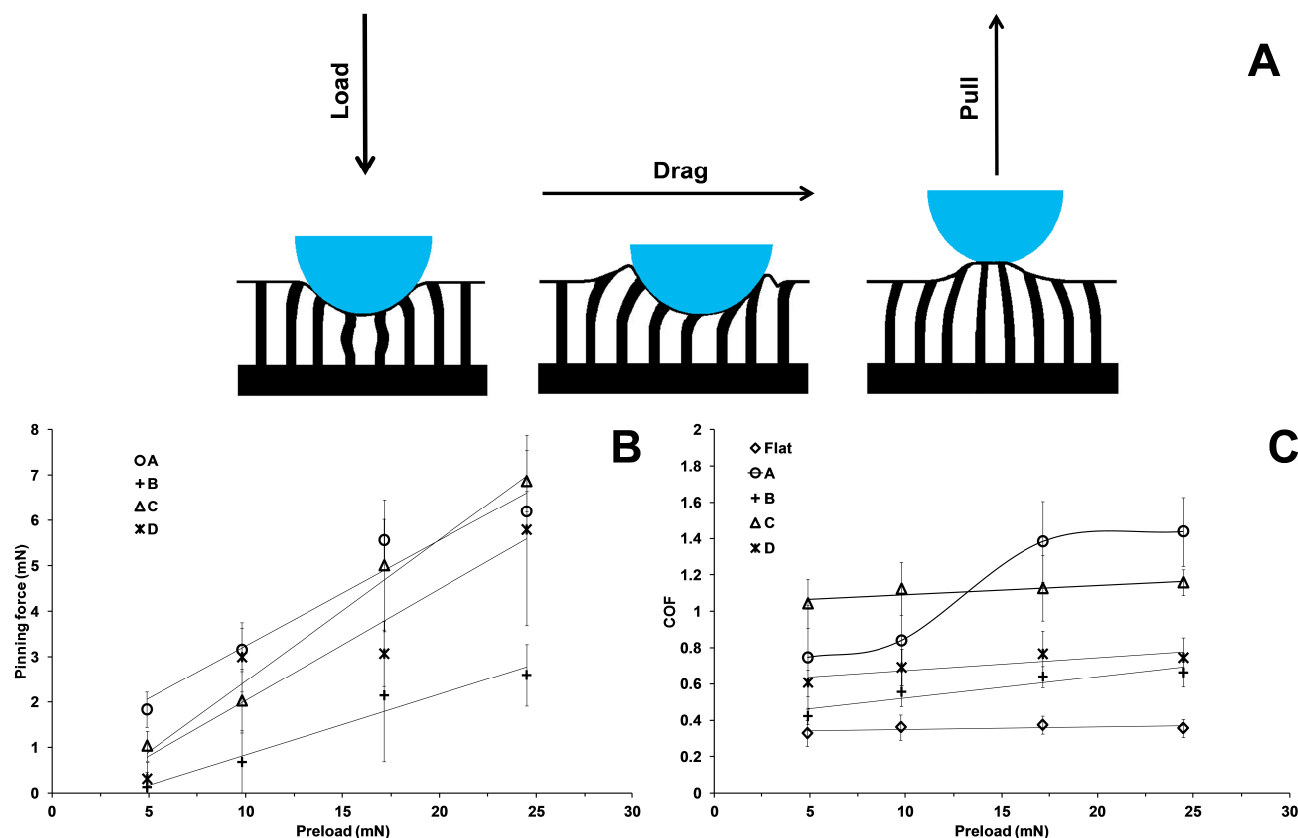


**Fig. S2** (A) Schematic of the three steps of load, drag, and pull in a typical LDP test with a hemispherical fused silica probe (8 mm in diameter) on double-level Teflon AF nanopillars; (B) Pinning force (i.e., the amount of decrease in the absolute value of the normal force at the start of the dragging step in LDP tests) and (C) Static coefficient of friction (COF) for the flat control sample and nanopillars of 200 nm in diameter with different heights of approximately 5.5, 16, 37, and 45 µm (samples A, B, C, and D, respectively) at nominal preloads of 5, 10, 17.5, and 25 mN.

Fig. S1A shows the schematic of an indentation test and typical force traces (i.e., normal force vs. displacement) for all samples under the nominal preload of 50 mN. The measured ultimate penetration depths ( $L_{pd}$ ) of the fused silica probe in nanopillars as well as the flat control sample at different preloads are plotted in Fig. S1B. By using the probe penetration depth values ( $L_{pd}$ ) and considering the geometrical correlations of the probe in contact, the approximate apparent surface area at the contact zone ( $a_{con}$ ) was calculated by  $a_{con} = \pi L_{pd} (d' - L_{pd})$  where  $d'$  is the probe diameter (see Fig. S1C).<sup>3</sup> It can be seen in Fig. S1C that the change of the surface area with preload within the applied preload range of ~5–50 mN is almost linear for all samples, including the double-level nanopillars and the flat control sample. Using the calculated apparent contact areas, the adhesion strength (pull-off force per unit surface area) for hierarchical nanopillars at different preloads has been calculated (Fig. S1D). The plot in Fig. S1D was used to calculate the maximum adhesion strength and the corresponding pull-off force for nanopillars of different geometrical properties.

According to Lifshitz theory, the Hamaker constant between phase 1 (fused silica probe) and phase 2 (Teflon AF) interacting across the medium 3 (air) can be calculated by<sup>4</sup>

$$A_{132} \approx \frac{3}{4} kT \left( \frac{\varepsilon_1 - \varepsilon_3}{\varepsilon_1 + \varepsilon_3} \right) \left( \frac{\varepsilon_2 - \varepsilon_3}{\varepsilon_2 + \varepsilon_3} \right) + \frac{3h\vartheta_e}{8\sqrt{2}} \frac{(n_1^2 - n_3^2)(n_2^2 - n_3^2)}{(n_1^2 + n_3^2)^{\frac{1}{2}}(n_2^2 + n_3^2)^{\frac{1}{2}} \{(n_1^2 + n_3^2)^{\frac{1}{2}} + (n_2^2 + n_3^2)^{\frac{1}{2}}\}} \quad (S2)$$

where  $k$  is the Boltzmann constant,  $T$  the temperature (~298 K),  $h$  the Planck's constant, and  $\vartheta_e$  the plasma frequency of the free electron gas (typically in the range of  $(3\text{--}5) \times 10^{15} \text{ s}^{-1}$ ).  $\varepsilon_1$ ,  $\varepsilon_2$ , and  $\varepsilon_3$  are the corresponding dielectric constants of phase 1, phase 2, and medium 3, and  $n_1$ ,  $n_2$ , and  $n_3$  are the refractive indices of phase 1, phase 2, and medium 3, respectively. Considering that  $\varepsilon_1 = 3.8$ ,  $n_1 \approx 1.448$ ,<sup>2</sup>  $\varepsilon_2 = 1.93$ ,  $n_2 \approx 1.31$ ,  $\varepsilon_3 = 1$ , and  $n_3 = 1$ ,<sup>4</sup> the Hamaker constant for the fused silica probe in contact with a flat Teflon AF surface would be approximately equal to  $5.64 \times 10^{-20} \text{ J}$  at 298 K.

The schematic of an LDP test on double-level nanopillars is shown in Fig. S2A. In the LDP tests, at the start of dragging the probe over the nanopillars, a rapid substantial decrease in the absolute value of the loading force (i.e., the normal force) was detected. The absolute value of this decrease (called “pinning force”) at different preloads, for all hierarchical nanopillars, has been plotted in Fig. S2B. The pinning force for the flat sample was not detected; for nanopillars, it was significant and increased linearly with preload. The static coefficient of friction (COF) values for all hierarchical nanopillars as well as for the flat control sample at different preloads are plotted in Fig. S2C. The measured static COF at the onset of dragging quantifies the force required to initiate the motion divided by the actual force pressing the probe over the nanopillars. The static COF for the flat surface was constant, as expected, but that of the nanopillars increased with increasing the preload (see Fig. S2C); overall, the COF values were remarkably higher than those of the flat surface.

Due to the fibrillar structure of the nanopillars, measuring the surface charge density during the tests by means of *in-situ* methods, such as those proposed by Smith,<sup>5</sup> and further used to concurrently measure the surface charge density and force in tribological tests,<sup>5-7</sup> is impractical. On the other hand, measuring the surface charge density by conventional methods, such as using a Faraday cup,<sup>8,9</sup> or by indirect chemical methods, as that proposed by Liu and Bard,<sup>10</sup> is not practical either and, even if possible, it cannot be very accurate because of the very small area of contact (< 0.5 mm<sup>2</sup>).

## References

- 1 K. Autumn, C. Majidi, R. E. Groff, A. Dittmore and R. Fearing, *J. Exp. Biol.*, 2006, **209**, 3558-3568.
- 2 J. Scheirs, in *Modern Fluoropolymers: High Performance Polymers for Diverse Applications*, John Wiley & Sons, Chichester, 1997.
- 3 M. P. Murphy, S. Kim and M. Sitti, *ACS Appl. Mater. Interfaces*, 2009, **1**, 849-855.
- 4 J. N. Israelachvili, in *Intermolecular and Surface Forces*, Elsevier Academic Press, London, 1991.
- 5 D. T. Smith, *J. Electrostat.*, 1991, **26**, 291-308.
- 6 R. G. Horn and D. T. Smith, *Science*, 1992, **256**, 362-364.
- 7 R. G. Horn, D. T. Smith and A. Grabbe, *Nature*, 1993, **366**, 442-443.
- 8 J. Lowell and A. C. Rose-Innes, *Adv. Phys.*, 1980, **29**, 947-1023.
- 9 W. R. Harper, in *Contact and Frictional Electrification*, Oxford University Press, London, 1967.
- 10 C. Liu and A. J. Bard, *Nat. Mater.*, 2008, **7**, 505-509.